Circularly polarised MIMO tapered slot antenna array for C-band application

S. Karamzadeh✉ and M. Kartal

A novel configuration of a multiple-input multiple-output (MIMO) circularly polarised (CP) antenna array operating in the C-band is presented. The array consists of 2 × 2 antipodal tapered slot antenna elements created in the sides of a rectangular as the rectangular grid that supplies a broadband impedance bandwidth and high gain array. To provide broadband MIMO with polarisation diversity, the antenna uses a dual-port feed network consisting of couplers, a crossover and delay lines which the diversity of polarisation changed by input ports.

Introduction: In recent years, antenna arrays have been widely used in radar and microwave communications because of their high gain, good directivity and extensive coverage area [1]. The main problem regarding the performance of array technology is the limited space available at each end of the communication link. The multiple-input multiple-output (MIMO) antenna with polarisation diversity has the ability to solve this problem. In a MIMO antenna, a physical antenna with different polarisation diversities has the same transmit and receive roles. Hitherto, in most papers [2–4], a change in the orthogonal polarisation has been proposed to overcome this problem. However, to resolve other problems such as combating multi-path interferences or fading, the Faraday rotation effect due to the ionosphere, and strict orientation between transmitting and receiving antennas, the use of a circularly polarised (CP) antenna is inevitable. In [5, 6], by utilising reconfigurable structures, polarisation diversity CP antennas could be achieved. However, the employment of active components such as *pin* diodes causes a decrease in bandwidth (BW), an increase in insertion loss and cost, and the addition of phase shift in array feed networks. In this Letter, a broadband MIMO antenna array with innovations such as: (i) a broadband feed network that consists of 90° and 180° couplers, a crossover and delay lines that provide the CP antenna with the ability to change right-hand CP (RHCP) and left-hand CP (LHCP) (polarisation diversity) by input choice; and (ii) 2 × 2 tapered slot antenna (TSA) array elements arranged in a square or rectangular grid configuration that supply the high gain antenna in a wide frequency BW with low mutual coupling, is presented.

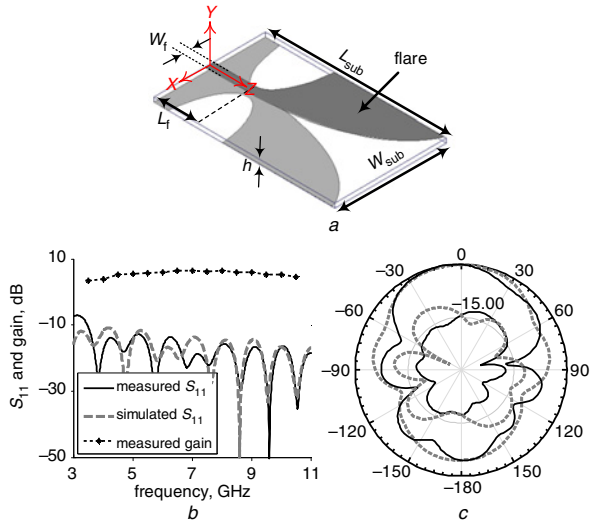

Fig. 1 *TSA configuration and results*

a Configuration of TSA
b Comparison between simulated and measured S_{11} (dB) and measured gain (dBi)
c Normalised measured pattern of antenna at 5.5 GHz (dashed line: co- and cross-polarisation of *E*-plane; solid line: co- and cross-polarisation of *H*-plane)

Single element: The configuration of the proposed antenna element is shown in Fig. 1*a*. The element is printed on an inexpensive FR4-epoxy laminate which has a thickness h of 0.8 mm with a manufacturer's-specified dielectric constant ε_r of 4.4 and loss tangent tanδ of 0.024. The radiating element configuration consists of an elliptical taper profile in the upper and bottom layers. W_{sub} is the width of the antenna and (L_{sub}–L_f) is the length of the taper profile (flare). The taper curves are obtained by [7].

To improve the impedance matching between the microstrip feed line of width W_f and the TSA and to avoid the balanced to unbalanced transformer, two half elliptic slots in the top and bottom flares are employed. The optimised antenna dimensions are: $R = 0.52$ mm, $W_f = 1.5$ mm, $W_{sub} = 40$ mm, $L_f = 15$ mm, $L_{sub} = 65$ mm and $h = 0.8$ mm.

The simulated and measured S_{11} of the TSA are presented in Fig. 1*b*. The measured BW is 103.4% (3.5–11 GHz) and the simulated BW of the TSA is 114.3% (3–11 GHz). The measured gain of the antenna is also shown in Fig. 1*b* with a maximum value of 8.6 dBi at a 7 GHz frequency. The normalised measured pattern of the antenna at 5.5 GHz is shown in Fig. 1*c*. The antenna pattern is end-fire with a half-power beamwidth of 76° and cross-polarisation of <−12 dB of co-polarisation.

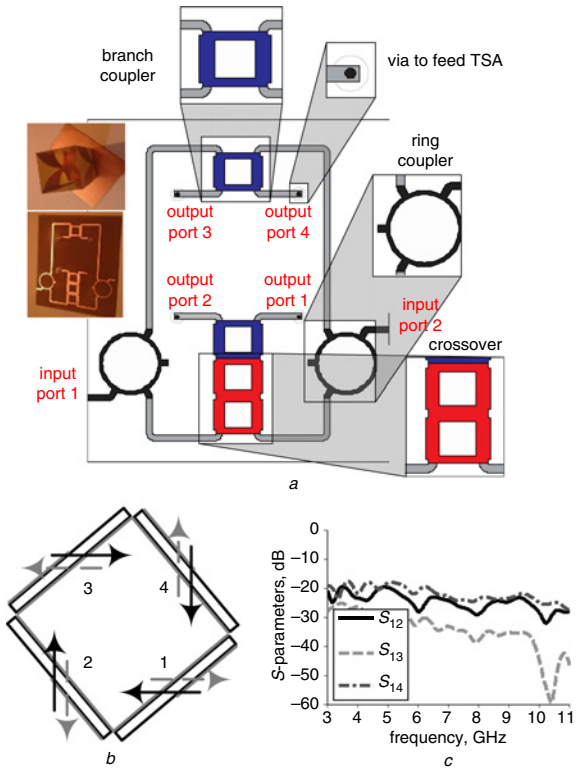

Fig. 2 *Overall structure of antenna array and feed network with mutual coupling results*

a Feed network of polarisation diversity in MIMO array
b Methods of arrangement in TSA array (phase variation: solid line is RHCP of port 1; dashed line is LHCP of port 2)
c Simulated mutual coupling between TSA elements

Feed network and MIMO array configuration: To attain a MIMO array with pattern diversity, a novel two-input and four-output port feed network is designed. As shown in Fig. 2*a*, the MIMO array feed network consists of two rate-race ring couplers, two branch line couplers and a crossover. The MIMO feed network employs two 180° ring hybrid couplers to achieve a −3 dB equal magnitude power split with 180° phase shifting. Two supplementary branch-line hybrid couplers then divide the signal energy into two paths and give the signal to each of the output branches with the same amplitude and 90° phase shifting [1]. To attain phase sequential rotation, between the ends of one side of the ring couplers and the branch line coupler, a crossover is embedded. The created phase shift by the crossover is compensated by a line length placed on the other side. The results of this arrangement of the components for each input port, based on the designed structure mentioned above, are given in Table 1. As is well known, CP waves are generated by exciting two or more orthogonal linearly polarised modes in equal amplitude, but in phase quadrature [1] (see Fig. 2*b*).

Table 1: Distribution of phase difference between TSA elements by each input port and type of generated diversity

P = port	Output P1	Output P2	Output P3	Output P4	Diversity
Input P1	$0 + \theta$	$90 + \theta$	$180 + \theta$	$270 + \theta$	RHCP
Input P2	$270 + \theta$	$180 + \theta$	$90 + \theta$	$0 + \theta$	LHCP

As reported, in the proposed MIMO array antenna structure, the exponential TSAs are arranged in a 2 × 2 rectangular grid configuration and are fed by metalised vias that isolate the TSA input impedance from the feed network impedance. The feed to feed spacing between the elements is 28.3 mm (0.51 $\lambda_{5.5GHz}$ – *wavelength in free space*). As shown in Fig. 2*c*, though the space between the TSAs is decreased, mutual coupling is reduced. The main reasons are (i) the surface current between the TSAs in this method of arrangement reduces and (ii) the TSA radiation pattern is end-fire.

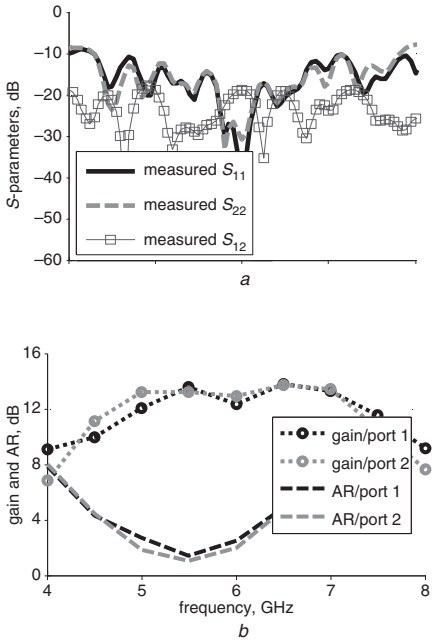

Fig. 3 *Comparison between simulated and measured results of MIMO array: measured S_{11}, S_{22} and S_{12} (Fig. 3a) and measured axial ratio and gain (Fig. 3b)*

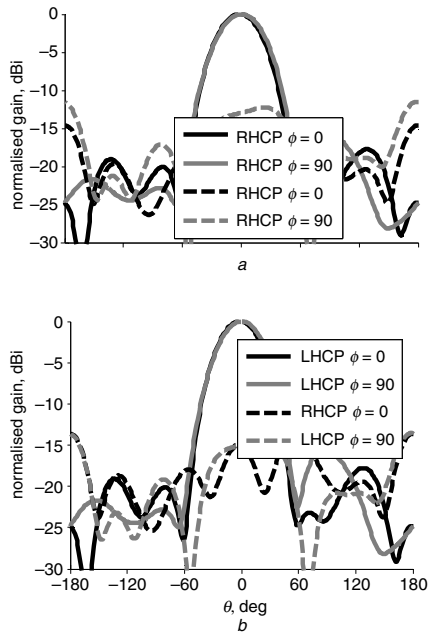

Fig. 4 *Normalised measured radiation pattern: for port 1 (Fig. 4a) and for port 2 (Fig. 4b)*

Result and discussion: The proposed TSA array was fabricated and measured using an 8722 ES Agilent vector network analyser. In Fig. 3*a*, the measured values of S_{11}, S_{12} and S_{22} are demonstrated. The measured BWs ($S_{11} < -10$ dB) for ports 1 and 2 are 60.8% (4.27–8 GHz) and 59.17% (4.26–7.84 GHz), respectively, and the mutual coupling between the two ports in the whole of the BW is <−17 dB. The measured 3 dB axial-ratio BW (ARBW) and gain of the proposed antenna for each input port are illustrated in Fig. 3*b*.

The measured 3 dB ARBW for ports 1 and 2 are 19.9% (4.98–6.08 GHz) and 24.8% (4.81–6.17 GHz), respectively. As illustrated in Fig. 3*b*, the maximum gain for port 1 is 13.87 dBic and for port 2 13.82 dBic. In the array design, the ground plane of the feed network on the other side of the substrate acts as a reflector for the TSA elements and as a result increases the gain of the antenna. That is why the gain of the proposed antenna is higher than the basis one which is TSA gain × array factor. The normalised measured radiation pattern of the proposed array at 5.5 GHz is shown in Fig. 4. As can be seen from Fig. 4, by exciting ports 1 and 2 the array antenna is radiated in RHCP and LHCP, respectively, and the polarisation diversity changes are significant. The design, when compared with the previous polarisation diversity array structures presented in Table 2, show significantly increased impedance BW and ARBW, i.e. the impedance and AR BW are, respectively, more than three- and two-fold wider than the previous designs.

Table 2: Comparison of proposed feed network structure and measured characteristics with other array antennas

Ref.	MePD	BW (freq. range) (GHz)	ARBW (freq. range) (GHz)	PG (dBic)
[5]	*pin* diode	0.82 (1.55–2.37)	0.31 (1.76–2.07)	~8
[6]	*pin* diode	0.11 (2.03–2.14)	0.01 (2.07–2.08)	~7
This work	Input port	3.58 (4.26–7.84)	1.36 (4.81–6.17)	~13.9

BW is the frequency range where VSWR ≤ 2; ARBW is 3 dB axial-ratio BW and MePD is method of changing polarisation diversity.

Conclusion: A novel design of a circularly polarised MIMO array antenna has been reported. The antenna element is designed and optimised to satisfy the expectations regarding BW, pattern and gain. Then the antenna array is configured with a novel feed network design. The array antenna with the feeding network gives improved gain and the desired CP diversity property, which is very important in some applications mentioned above. Another novelty of the designed array structure is the additional gain improvement obtained by the substrates acting as a reflector for other array elements.

Submitted: *4 June 2015* E-first: *12 August 2015*
doi: 10.1049/el.2015.1784
One or more of the Figures in this Letter are available in colour online.

S. Karamzadeh and M. Kartal (*Department of Electric and Electronics Engineering, Istanbul Technical University, Istanbul, Turkey*)

✉ E-mail: karamzadeh@itu.edu.tr

S. Karamzadeh: Also with the Department of Electric and Electronics Engineering, Istanbul Aydin University, Istanbul, Turkey

References

1 Karamzadeh, S., Rafii, V., Kartal, M., *et al.*: 'Circularly polarised array antenna with cascade feed network for broadband application in C-band', *Electron. Lett.*, 2014, **50**, (17), pp. 1184–1186, doi: 10.1049/el.2014.1147
2 Wang, L., Xu, L., Chen, X., *et al.*: 'A compact ultrawideband diversity antenna with high isolation', *IEEE Antennas Wirel. Propag. Lett.*, 2014, **13**, pp. 35–38, doi: 10.1109/LAWP.2013.2295414
3 Huang, H., Liu, Y., and Gong, S.: 'Uniplanar differentially driven UWB polarisation diversity antenna with band-notched characteristics', *Electron. Lett.*, 2015, **51**, (3), pp. 206–207, doi: 10.1049/el.2014.3626
4 Chacko, B.P., Augustin, G., and Denidni, T.A.: 'Electronically reconfigurable uniplanar antenna with polarization diversity for cognitive radio applications', *IEEE Antennas Wirel. Propag. Lett.*, 2015, **14**, pp. 213–216, doi: 10.1109/LAWP.2014.2360353
5 Cao, W., Zhang, B., Liu, A., *et al.*: 'A reconfigurable microstrip antenna with radiation pattern selectivity and polarization diversity', *IEEE Antennas Wirel. Propag. Lett.*, 2012, **11**, pp. 453–456, doi: 10.1109/LAWP.2012.2193549
6 Tsai, J.-F., and Row, J.-S.: 'Reconfigurable square-ring microstrip antenna', *IEEE Trans. Antennas Propag.*, 2013, **61**, (5), pp. 2857–2860, doi: 10.1109/TAP.2013.2244554
7 Langley, J.D.S., Hall, P.S., and Newham, P.: 'Balanced antipodal Vivaldi antenna for wide bandwidth phased arrays', *IEEE Proc., Antennas Propag.*, 1996, **143**, (2), pp. 97–102